JOURNAL OF CATALYSIS 130, 181–191 (1991)

Influence of Ceria on the Interaction of CO and NO with Highly Dispersed Pt and Rh

P. LÖÖF,* B. KASEMO,* S. ANDERSSON,† AND A. FRESTAD†

*Physics Department, Chalmers University of Technology, S-412 96 Gothenburg, Sweden; and †Emissionsteknik AB, S-42131 V. Frölunda, Sweden

Received January 29, 1990; revised February 12, 1991

TPD spectra of CO and NO were studied at atmospheric pressure for highly dispersed Pt, Rh, and Pt + Rh supported on Al_2O_3, Al_2O_3 + ceria, and pure ceria, respectively. Ceria has a strong influence on the CO and NO spectra on the reduced catalysts, demonstrating that ceria modifies the catalyst properties. For NO nearly complete decomposition to N_2 takes place on all reduced catalysts at low NO doses, while product oxygen inhibits the decomposition. Ceria slows down this inhibition effect, probably due to oxygen spillover from the noble metal to reduced ceria. The activities for the $CO + \frac{1}{2}O_2 \rightarrow CO_2$ and $NO + CO \rightarrow \frac{1}{2}N_2 + CO_2$ reactions are both enhanced by the addition of ceria for stoichiometric reactant mixtures. The ceria-induced effects are associated with the interaction of highly dispersed noble metal with oxygen vacancies in the reduced ceria support.

1. INTRODUCTION

Metal-support interaction in catalytic reactions over supported metal catalysts has received considerable attention over the past years (*1–9*). Such interaction may, for example, consist of "doping" the support (usually a metal oxide) by individual metal atoms, or interaction between metal atoms in small clusters and the support. In this work we have investigated supported noble metal catalysts, of the type used in car exhaust catalysis, for such effects. The systems investigated were adsorption and reaction of NO and CO on highly dispersed Pt, Rh, and Pt + Rh, respectively, supported on Al_2O_3, ceria, and mixed Al_2O_3 + ceria. For earlier results on the role of ceria, see, e.g., Refs. (*3, 6*). The method of investigation was temperature-programmed desorption (TPD) and temperature-programmed reaction at 1 atm pressure in a flow reactor, on-line connected to a mass spectrometer (Falconer and Schwartz (*10*) have reviewed the use of these methods to study supported catalysts in flow reactors). The results from our study reveal significant metal-support interaction.

2. EXPERIMENTAL

2.1. Catalysts and Catalyst Preparation

The monolithic samples used in this study were prepared by coating a monolithic support (400 cpi, Corning) with high surface area washcoats, Al_2O_3 and Al_2O_3 + ceria. Pt, Rh, and Pt + Rh were then deposited on the samples. The Al_2O_3 powder (Puralox scfa 90) had a BET-area of 90 m^2/g and was obtained from Condea Chemi. X-ray diffraction measurements show that this Al_2O_3 mainly consists of θ-Al_2O_3 with contributions of γ-, α-, and δ-Al_2O_3. The Al_2O_3 + 20% ceria powder was prepared by incipient wetness impregnation using cerium nitrate ($Ce(NO_3)_3$, purity > 99%, Fluka AG) dissolved in deionized water. The wet powder was dried at 125°C and calcined for 2 h at 650°C in air. The Al_2O_3 powder and Al_2O_3 + ceria powder were then mixed with water and ball-milled to obtain a suspension suitable for the coating of the monolithic sup-

0021-9517/91 $3.00

port. The coated support (20 wt% washcoat of the total sample weight) was then dried at 125°C and calcined for 2 h at 500°C in air. Samples with 0.3 wt% Pt, 0.06 wt% Rh and 0.3 wt% Pt + 0.06 wt% Rh were then prepared by impregnation using the incipient wetness technique. The impregnation solution was H_2PtCl_6 or $RhCl_3$ dissolved in deionized water. The samples were then dried at 125°C and calcined for 2 h at 500°C in air. The weight, length, and diameter of the monolithic samples were 0.9 g, 28 mm, and 8 mm, respectively, for a carrier gas flow rate of 60 ml/min. When the carrier gas flow rate was 30 ml/min the weight and length of the samples were reduced by a factor of two.

Powdered high surface area ceria (107 m^2/g) was also used as a support. One wt% Pt and 1 wt% Rh were deposited on ceria powder using the same procedure as above. The weight of these samples was 1 g.

2.2. *Experimental System and Procedure*

The TPD experiments were performed in a quartz flow reactor described previously (*11*). The reactor with the sample is on-line connected to a mass spectrometer which continuously analyzes the composition of the gas. Gas is sampled by a quartz capillary-type probe (*12*) positioned about 4 mm downstream from the catalyst. The reactor cell can be heated with a linear temperature rise up to 1000 K by an external heating coil. An inert carrier gas (Ar) at atmospheric pressure flows continuously over the sample. The selected gas flow rates of the carrier gas were 60 ml/min and 30 ml/min for 0.9 and 0.45 samples, respectively. The catalyst temperature is measured by a 0.1-mm-diam chromel–alumel thermocouple in one of the channels of the monolithic sample, or inside the powder in the case of ceria powder samples. The gas composition of reacted and unreacted gas is measured with the mass spectrometer, which has been calibrated using known gas mixtures. At regular intervals control measurements were performed without a sample in the cell to eliminate the risk of wall reactions on catalyst remnants from earlier runs.

The gas mixtures used were high purity 4% CO in Ar, 4% H_2 in Ar, 4% NO in Ar, and 2% O_2 in Ar and 100% Ar, respectively (99.9997% purity). All measurements were performed at 1 atm.

The samples were always pretreated in the following way, prior to experiments. First the sample was oxidized in 2% O_2 in Ar for 5 min at 900 K to remove any carbon contamination. It was then reduced in 4% H_2 in Ar for the same time and temperature. Longer reduction times did not influence the observed TPD spectra. (Recent XPS results recorded after similar reductive treatment show that Pt is in metallic form after this treatment (*13*).) The reaction cell was thereafter flushed with pure Ar for 1 min and then cooled to room temperature over a period of 7 min. CO or NO was then adsorbed, either by pulse injection into the carrier gas (when a small amount of adsorbed gas was desired) or by continuous flow of the gas over the catalyst (when saturation uptake was desired).

After gas adsorption TPD runs were performed by heating the reaction cell by an external heating coil at a rate of 2 K/s. This rate was found to be an optimum compromise to avoid temperature gradients, to minimize readsorption effects, and to maximize the sensitivity. After CO adsorption the CO and CO_2 signals were continuously recorded during the TPD run, and after NO adsorption NO, N_2O, and N_2 signals were recorded.

3. RESULTS

3.1. *TPD of CO*

The catalyst was saturated with CO at room temperature in continuous flow of CO/Ar, before the TPD runs. Figures 1a–1c show TPD spectra of CO desorbing from reduced catalysts of Pt, Rh, and Pt + Rh supported on Al_2O_3 on a monolithic carrier. There are some significant differences between the Pt, Rh and Pt/Rh CO spectra but basically they consist of three overlapping

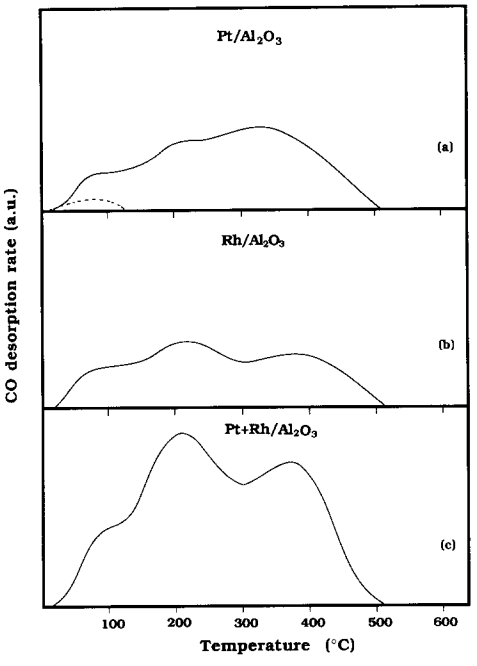

FIG. 1. TPD spectra of CO after CO adsorption at room temperature on Al_2O_3-supported, reduced catalysts. (a) Pt, (b) Rh, (c) Pt + Rh. Heating rate 2 K/s. The dashed curve in (a) is the background from the support alone.

contributions centered around 100, 200, and 350°C in the Pt case and 100, 200, and 400°C in the Rh and Rh + Pt cases. The amounts of desorbed CO in the three peaks are given in Table 1. Rh seems to dominate the mixed Pt/Rh catalyst since its TPD spectrum is very similar to the Rh/Al_2O_3 spectrum. The dashed curve shows the TPD spectrum from the blank Al_2O_3 and Al_2O_3 + ceria support (Al_2O_3 and Al_2O_3 + ceria without noble metal exhibit similar CO TPD spectra indicating that ceria is comparatively inactive toward CO adsorption).

In all CO TPD runs on Pt and/or Rh there is also a CO_2 signal (not shown) in the *T*-range 250–500°C, whose magnitude was around 10–15% of the CO signal.

In the following we focus on how the three spectra of Figs. 1a–1c change upon addition of ceria to the support.

Figures 2a–2c show the same type of spectra as those in Fig. 1 but with 20% ceria added to the Al_2O_3 support. The spectra are dramatically different, now consisting of two well-resolved peaks (in contrast to the three overlapping peaks in Fig. 1) around 80 and 470°C for both Pt, Rh, and Pt + Rh (the CO_2 signal is in this case about a factor of five lower than with pure Al_2O_3). The amounts of CO desorbed in each peak are given in Table 1. The broad double peak in the region 200–400°C observed in the absence of ceria (Fig. 1) is replaced by a peak around 470°C, indicating considerably stronger CO bonding. It is tempting to attribute these differences to the effect of ceria interaction with noble metal particles.

In order to test this idea samples were prepared by using pure ceria powder impregnated with Pt and Rh, respectively. TPD spectra of CO from such samples, pretreated in the same way as the monolithic samples, are shown in Figs. 3a and 3b. They show basically the same features as the spectra from the mixed Al_2O_3 + ceria support. This observation verifies that CO

TABLE 1

Amounts of Desorbed CO and Peak Temperatures for the CO TPD Peaks

Catalyst	CO desorption (μmol/g)		
	Peak 1 100°C	Peak 2 200°C	Peak 3 350–400°C
Rh/Al_2O_3	0.4	1.1	1.0
Pt/Al_2O_3	0.4	0.8	1.5
PM/Al_2O_3	0.7	2.4	2.1
		Peak 1 80°C	Peak 2 470°C
Rh/Al_2O_3 + ceria		0.4	2.1
Pt/Al_2O_3 + ceria[a]		0.4	1.9
PM^b/Al_2O_3 + ceria[a]		0.7	3.9

[a] Between peak 1 and 2 there is a broad contribution of desorbing CO. The amount of desorbed CO in this region is 0.4 and 0.6 μmol/g from Pt and PM containing samples, respectively.

[b] PM stands for precious metals (Pt,Rh).

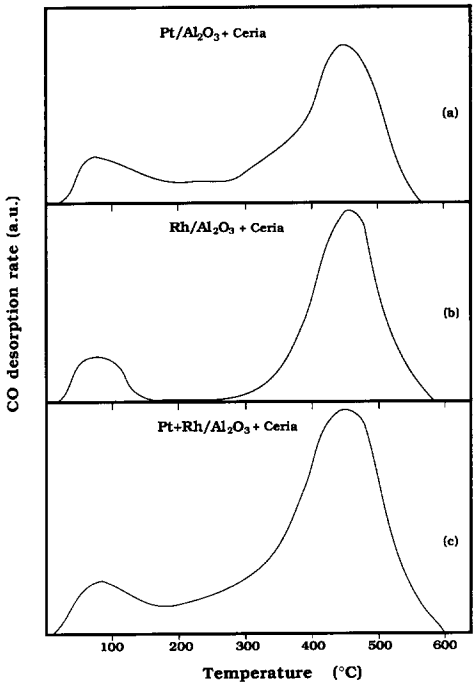

FIG. 2. TPD spectra after CO adsorption at room temperature on reduced, Al_2O_3 + ceria-supported catalysts. Heating rate 2 K/s. (a) Pt, (b) Rh, (c) Pt + Rh. Support background approximately as in Fig. 1a.

adsorption on highly dispersed Pt and Rh particles supported on ceria are strongly influenced by the ceria support.

There are some minor differences between the TPD spectra from Pt and Rh, respectively, in Figs. 2 and 3. The Pt/Al_2O_3 + ceria spectrum (Fig. 2a) has, in addition to the two peaks, a broad contribution in the T-region between the peaks, while with pure Rh this contribution is absent. For the mixed catalyst (Fig. 2c) it is present but not when Pt is deposited on pure ceria. These observations suggest that this contribution is due to Pt deposited on Al_2O_3 regions with no ceria present. Rh thus seems to be deposited preferentially with ceria. Another difference between Pt and Rh is that the high-temperature peak has a higher relative intensity in the Rh TPD spectra than in the Pt spectra (most obvious in Fig. 3).

For comparison with the data presented above, samples with additions of La_2O_3 or ZrO_2 to Pt,Rh, and Pt + Rh on Al_2O_3 were also prepared and tested. The addition of these substances did not change the TPD spectra of the type shown in Fig. 1, indicating that La_2O_3 and ZrO_2 do not interact in the same way as ceria with the noble metals.

An important quantity in this context is the dispersion (i.e., the "size") of the noble metal particles. The dramatic influence of the ceria support would be difficult to understand unless the noble metal dispersion is very high, since large particles would be "bulk like" and unaffected by the support, except possibly within a few atomic distances from the point of contact between the metal particle and the support. The dispersion can be obtained by CO adsorption/desorption runs since the total amount of noble metal in the catalyst is known, and since the gas flow rate and absolute CO concentration in the gas flow during a TPD run are measured quantitatively. The total amount of CO desorbed is obtained from the area under the TPD curves in Figs. 1–3. Assuming a saturation uptake of CO on Pt and Rh of 0.7 CO molecules per metal atom (which is close to the value observed for many CO–metal single crystal systems in-

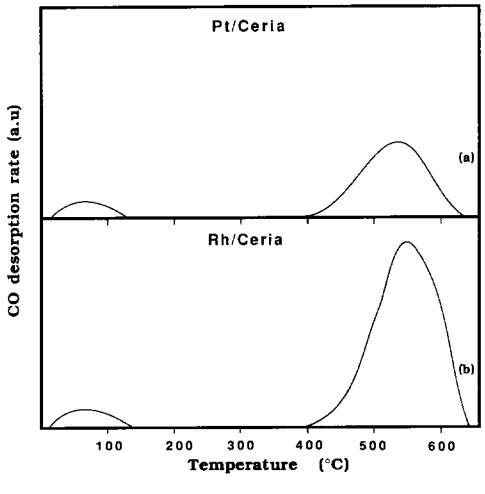

FIG. 3. TPD spectra of CO after CO adsorption on (a) Pt and (b) Rh supported on pure ceria powder. The catalysts were reduced in H_2 prior to adsorption.

cluding the catalytically active noble metals (*14*)), we obtain dispersion values for the Pt, Rh, and Pt–Rh samples of Fig. 1 of 25, 60, and 35%, respectively, and similar dispersion values for the samples of Figs. 2a–2c. The chosen chemisorption stoichiometry of 0.7 CO per noble metal atom may be debated, and is probably larger at high dispersion due to the occurrence of larger CO/metal ratios, e.g., dicarbonyl CO, on small clusters. This means that the dispersion values may be smaller than given above but they are still high enough to enable direct metal-support interaction. Thus the dispersion is very high, the particles are very small, and a large fraction or all of the noble metal atoms are within a few atomic distances from the ceria support, which makes direct metal-support interaction possible.

It should be emphasized that these results are observed on reduced, fresh catalysts with high dispersion. Under these conditions there is obviously a strong influence on the CO–noble metal interaction from the ceria support. We do not claim that these effects are necessarily present or as strong under real car exhaust catalyst operation where the dispersion is usually much lower and the catalyst normally less reduced.

3.2. *TPD of NO*

Due to an observed slow adsorption of NO on the Al_2O_3 support, interfering with the adsorption on the noble metal (to be described in detail in a separate paper (*15*)), the NO adsorption/desorption runs had to be made by pulse injection into the Ar carrier gas. By careful dosing, the signal from the support could be kept negligible in comparison with the signal from NO adsorbed on the noble metal particles. The pulse was chosen so that most of the NO in the pulse was adsorbed by the catalyst, and only a negligible amount was transmitted through the catalyst, as determined by the MS signal for NO accompanying the pulse injection. In all cases a small instantaneous N_2 signal accompanied the NO pulse injection indicating a small spontaneous NO dissociation +

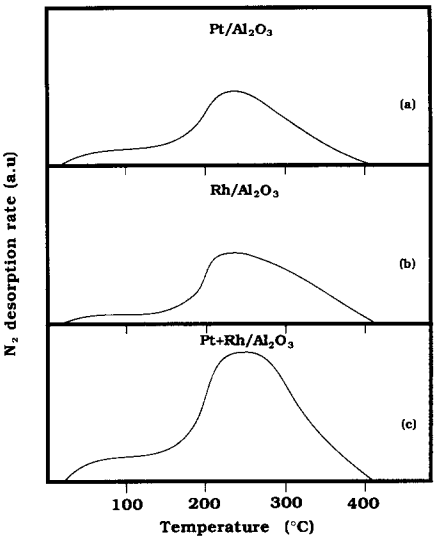

FIG. 4. TPD spectra of N_2 after NO adsorption on Al_2O_3 supported, reduced catalysts at room temperature. (a) Pt, (b) Rh, (c) Pt + Rh. No or only weak NO and N_2O desorption was observed. Desorption from the support is negligible.

N_2 desorption already at room temperature. This effect was more pronounced with Rh than with Pt and Pt + Rh catalysts. Addition of ceria of the catalysts enhanced this effect (a similar effect was also seen with pure reduced ceria samples without deposited noble metal).

Figures 4a–4c show the N_2 signal recorded during linear heating (2 K/s) of three samples after adsorption of NO at room temperature. The three samples were similar to the ones used to record Figs. 1a–1c for CO; i.e., they were reduced prior to adsorption and consisted of Pt, Rh, and Pt + Rh deposited on Al_2O_3 on monolithic samples. The spectra of Fig. 4, which serve as a reference for results presented below, show a minor N_2 desorption plateau around 100°C and a major N_2 desorption peak centered around 220–240°C. Only very weak or no NO and N_2O desorption were observed, demonstrating the almost complete decomposition of NO via $2NO \rightarrow N_2 + 2O$. (The oxygen atoms are deposited on the catalyst.) No major differences in the product distri-

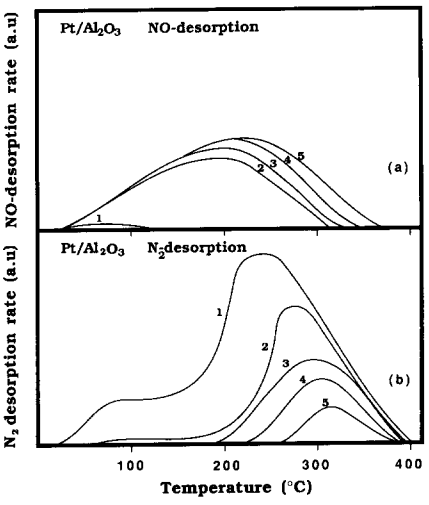

FIG. 5. Successive TPD runs of N_2 and NO after NO adsorption–desorption runs on Pt/Al_2O_3. No or only weak N_2O desorption was observed. The first run was made on a reduced catalyst. No reduction between successive runs. The decline in the N_2 signal and concerted rise in the NO signal are due to the inhibiting effect of oxygen on NO dissociation.

bution were observed between Pt, Rh, and Pt + Rh.

The results of Fig. 4 are obtained only with carefully reduced samples. If the experiment of Fig. 4a is repeated several times in succession, without reduction in between, the NO decomposition becomes incomplete. (After the desorption run the sample was cooled to RT, and NO was adsorbed again and followed by a new TPD run). Figure 5 shows the result of five such successive runs. Only the spectrum for Pt/Al_2O_3 is shown since the behavior of Rh and Pt + Rh are similar. The upper panel shows the NO desorption rate and the lower panel the N_2 desorption rate. It is clearly seen how the N_2 signal decreases and the NO signal increases after each run demonstrating that the oxygen atoms deposited after each run inhibits the capacity of the catalyst to decompose NO.

The passivation of the catalyst (with respect to NO decomposition) is considerably slower than would be expected if all oxygen atoms from decomposed NO were only deposited on the surface of noble metal particles. In the latter case we estimate that only one or a few NO adsorption/desorption runs should be required for complete passivation, which is not the case. This suggests that the oxygen atoms either move to neighboring Al_2O_3-support sites via a spillover effect, or alternatively are incorporated in the bulk of the noble metal particles. The spillover effect may occur but two observations indicate that the latter process is important. First, the passivation was found to be faster for samples with a higher noble metal dispersion. Second, oxidation/reduction runs of a 0.3 wt% Pt/Al_2O_3 sample, where oxidation was performed in O_2 at 600°C and reduction was performed in CO, showed an integrated CO_2 production in the reduction run corresponding to an O/Pt ratio of 1.5. Both observations are consistent with partial bulk oxidation of the Pt particles.

The addition of ceria to the alumina support has, as in the CO case, a dramatic effect on the TPD desorption spectra (Fig. 6). The

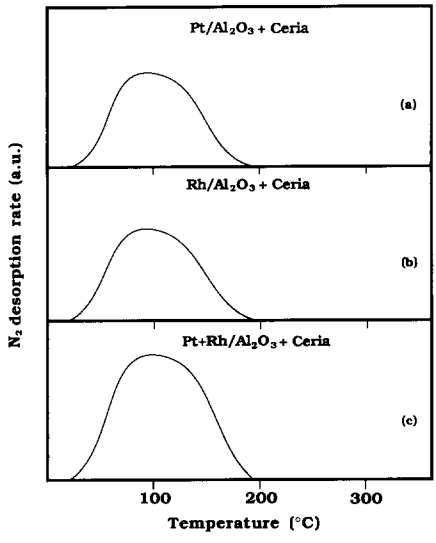

FIG. 6. TPD spectra of N_2 after NO adsorption at room temperature on reduced, Al_2O_3 + ceria-supported catalysts. (a) Pt, (b) Rh, (c) Pt + Rh. No or only weak NO and N_2O desorption was observed. Desorption from the support is negligible.

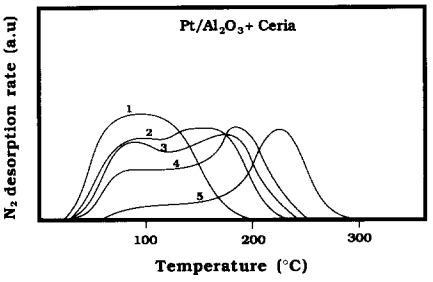

FIG. 7. Successive TPD runs of N_2 and NO after NO adsorption at room temperature on a Pt/Al_2O_3 + ceria catalyst. No or only weak N_2O desorption was observed. The first run was made on a reduced catalyst. No reduction was made between successive runs.

main desorption peak, which in the absence of ceria was peaked around 220–240°C, now has its peak intensity around 100°C and nearly no N_2 signal is detected at 220–240°C. Since N_2 desorption was also observed at nearly the same temperature (80°C) after NO adsorption on a reduced, blank Al_2O_3 + ceria support and on pure reduced ceria, the 100°C peak can be a mixture of desorption from ceria and from noble metal. However, comparing the absolute amount of desorbed N_2 from the noble metal/Al_2O_3 and Al_2O_3/ceria samples we conclude that more than 60% of the total desorption yield for the noble metal/Al_2O_3 + ceria samples must derive from the noble metal. These observations are strong evidence that the change in the N_2 desorption spectra upon ceria addition is due to interaction between the noble metals and ceria in the samples, and not just to the ceria support itself.

Figure 7 shows the result of five successive NO adsorption/desorption runs, like the ones in Fig. 5, but now with Pt deposited on Al_2O_3 + ceria. Only the spectrum for Pt/Al_2O_3 + ceria is shown since the spectra with Rh and Pt + Rh are very similar. Ceria has three effects in comparison with the results of Fig. 5. (i) As discussed above, the main N_2 peak appears at lower temperature. (ii) As successive runs are performed and oxygen is accumulated on the catalyst (compare with Fig. 6) the main N_2 peak moves to higher temperature, eventually almost to the temperature observed with no ceria present. (iii) The oxygen-inhibiting effect on NO decomposition is much slower when ceria is added (i.e., larger oxygen doses are required to inhibit NO decomposition). The latter is most easily understood in terms of oxygen spillover from the noble metal to the reduced ceria.

The dispersion values obtained from the TPD runs with NO on Pt, Rh, and Pt + Rh supported on Al_2O_3 were 25, 70, and 40%, respectively, in good agreement with the values obtained with CO (previous section). In this determination we have assumed the same saturation density of NO as for CO, i.e., 0.7 NO per noble metal atom. The total number of adsorbed NO on reduced samples was determined as twice the number of desorbed N_2 molecules. There is of course the same uncertainty in the NO/metal ratio as with CO. The dispersion values may thus be somewhat smaller. Dispersion values for samples with Al_2O_3 + ceria supports could not be exactly determined with NO because of the above mentioned effect that reduced ceria contributes to NO decomposition.

The samples containing La_2O_3 or ZrO_3 were also tested with NO. The same results as with the pure Al_2O_3 support was obtained, indicating that there is no interaction between the noble metals and La_2O_3 or ZrO_2 of the kind found with ceria.

3.3. Reaction Kinetics

A few measurements were made on the activity of the various catalysts for the $CO + \frac{1}{2}O_2 \rightarrow CO_2$ and $CO + NO \rightarrow CO_2 + \frac{1}{2}N_2$ reactions. These measurements were less detailed than the TPD measurements and we only emphasize the main trends in the former data. Only stoichiometric gas mixtures were used. The same catalysts as for the TPD runs were used and they were pretreated as for the TPD runs. As a measure of the activity of the catalysts two different quantities are used, namely (i) the temperature, T_{50}, where 50% of the reactants are converted to products, and (ii) the average

TABLE 2

Summary of results for the reactions $CO + \frac{1}{2}O_2 \rightarrow CO_2$ and $CO + NO \rightarrow \frac{1}{2}N_2 + CO_2$. T_{50} is the temperature (in °C), where 50% conversion occurs. E_a (kJ/mol) is obtained from the slope of Arrhenius plots in the low T regime prior to "ignition."

	$CO + \frac{1}{2}O_2$		$CO + NO$	
Catalyst	T_{50}	E_a	T_{50}	E_a
Pt/Al_2O_3	200	20	230	53
Pt/Al_2O_3 + ceria	100	27	150	30
Rh/Al_2O_3	—	—	—	—
Rh/Al_2O_3 + ceria	85	50	110	37
PM/Al_2O_3	150	30	200	20
PM/Al_2O_3 + ceria	100	40	115	40

slope of Arrhenius plots in the kinetically controlled regime, prior to ignition. The results are listed in Table 2. (The reference point for Rh/Al_2O_3 is quantitatively lacking but T_{50} was higher for this catalyst than for Rh/Al_2O_3 + ceria.) The most important observation, in line with the TPD results, is that ceria has a significant effect on both reactions for Pt, Rh, and Pt + Rh catalysts. The T_{50} values for the CO oxidation reaction on all ceria-containing samples are lower than in the absence of ceria. For the CO + NO reaction on Rh- and ceria-containing samples the same correlation exists. The quoted activation energies should only be taken as relative measures of the T-dependences of the activity in the regime prior to ignition, because of the low conversion at low temperature and the narrow T-regime over which these values were determined.

4. DISCUSSION

4.1. CO

We first discuss the TPD spectra for CO on Pt, Rh, and Pt + Rh supported on alumina and then the changes in the spectra when ceria is added. With pure Al_2O_3 as the support the TPD spectra (Fig. 1a–1c) are characterized by three overlapping peaks centered around 100, 200, and 350–400°C, respectively, for Pt, Rh, and their mixture. Based on the numerous IR studies on supported Rh catalysts (*16–20*) the three peaks may be associated with different CO–noble metal bond geometries; linear, bridge bonded, and dicarbonyl CO. The latter has been attributed to CO bound to atomically dispersed noble metal (*16*). Dictor and Roberts (*16*) found the dicarbonyl species to be the only one stable above 200°C. The high-temperature peak might therefore be attributed to a dicarbonyl species. The assignment of the peak is, however, uncertain. A second possibility which cannot be ruled out is that CO dissociates (as suggested in Ref. (*21*)) and then desorbs by C + O recombination during the TPD run.

The TPD spectra change significantly upon ceria addition. The middle peak vanishes (or shifts to considerably higher temperature) and the high-temperature peak appears around 500°C, i.e., about 100–150°C higher than in absence of ceria. The high-temperature peak may be due to a new type of CO bonding, as suggested from studies of $CO/Rh/SiO_2$ with and without ceria (*17*) and $CO/Pd/SiO_2$ with and without alkali metal (*18*). A new IR absorption band was observed at 1725 cm^{-1} when ceria was added to the former type of structure. For the latter type of catalyst a new absorption band was observed at about 1800 cm^{-1}. This CO species was more strongly bound to the surface than other types of CO, as judged from its thermal stability. The new IR absorption bands were in both cases attributed to CO bound via both its carbon and oxygen atoms. In line with this interpretation we tentatively attribute the high-temperature peak, appearing in the presence of ceria, to CO species where the carbon atom is bound to the edge atoms of small noble metal particles and where the oxygen atom is bound to oxygen vacancies in the adjacent, reduced ceria support. It cannot be excluded that the high-temperature peak has contributions from an increased amount of dicarbonyl species, when ceria is added to the catalyst.

The pronounced difference between the TPD spectra with and without ceria is at variance with the work of Oh and Eickel (*6*) for CO on Rh/Al_2O_3 and $Rh/ceria/Al_2O_3$. Their TPD spectra were for both types of samples relatively similar to our spectra from Rh on Al_2O_3, i.e., a broad structure over the 50–500°C range (although our spectra contain more structure). Addition of ceria did not cause significant differences in their TPD spectra. Oh and Eickel also performed IR measurements on the two types of samples and in line with the TPD results they observed no difference in the CO IR spectra. Jin *et al.* (*22*) observed TPD spectra for CO/Pt/ceria that are similar to our $CO/Pt/Al_2O_3$ spectra.

We see no obvious explanation for these differences in results. However, there are several differences in the experimental conditions. One possibility is that the higher reduction temperature used in our work (600°C) in comparison with those of Oh and Eickel (450°C) and Jin *et al.* (550°C) resulted in different oxidation status of the samples. Jin *et al.* and Oh and Eickel used much lower gas pressures, 10^{-4} Torr, and gas exposures than in the present work.

The ceria-related effect is very sensitive to oxygen. Repeated CO TPD runs reduced the ceria effect and made the spectra more and more similar to the noble metal/Al_2O_3 spectra. This was attributed to trace amounts of oxygen in the feed gas. A second difference between our experiments and those of Oh and Eickel and Jin *et al.* may be that the noble metal dispersion was higher in our case. Jin *et al.* estimated a mean particle size of 13 nm, corresponding to much lower dispersion than in our samples. The samples studied by Oh and Eickel had a dispersion lower than that of our samples by a factor of only about two.

A comment is required on the small CO_2 signal in the CO TPD spectra. It may be attributed to remaining oxygen in the catalyst after reduction and/or trace amounts of O_2 in the feed gas, which upon CO exposure oxidize CO to CO_2. A simple calculation based on the known gas impurity (3 ppm) showed that the O_2 impurity explanation is feasible. The formed CO_2 is then probably adsorbed on the support, since the CO_2 signal does not affect the amount of CO that can be adsorbed/desorbed by the noble metals. CO_2 later desorbs during the TPD run (the adsorption properties of the Al_2O_3 support toward CO_2 is to be described in a separate paper (*14*)). Contribution to the CO_2 signal from disproportionation of CO was ruled out since no CO_2 signal was observed during inlet of oxygen into the feed gas at 900 K directly after the TPD run (carbon formed by a disproportionation reaction would have been oxidized to CO_2 during the oxygen exposure).

Concerning the CO oxidation kinetics we found essentially the same results as both Oh and Eickel (*6*) and Summers and Ausen (*3*), namely that ceria has a positive effect on the activity. However, our study was in this respect much less detailed than the other two studies.

4.2. NO

Ceria on a reduced catalyst has a strong influence on the NO–noble metal interaction. In contrast to CO, NO decomposes nearly completely on both the Al_2O_3 and Al_2O_3 + ceria-supported noble metal catalysts, when they are reduced. The N_2 desorption occurs at lower temperature (100°C) with ceria in the support than with pure Al_2O_3 (220–240°C), indicating either a lower activation energy for NO dissociation or a lower activation energy for N_2 desorption or both when ceria is present. Similar results have been obtained for NO on Rh/Al_2O_3 and Rh/Al_2O_3 + ceria by Oh and co-workers (*23*). However, they observed a lesser degree of NO dissociation and the effect of ceria was less pronounced compared to our findings. In their work the addition of ceria caused an increase of the low-temperature N_2 peak and left the high-temperature N_2 peak vitually unchanged. These differences could be due to a more complete reduction of our samples. The latter as-

sumption is based on the observation that samples on which oxygen has been deposited, e.g., by repeated NO TPD runs, exhibit a lower degree of NO dissociation and also, in the case of ceria-containing samples, the appearance of two N_2 peaks.

NO dissociation occurs also on blank, reduced Al_2O_3 + ceria and on pure ceria supports with an N_2 desorption peak around 80°C. It was, however, concluded (Section 3.2) that the amount desorbed in the absence of noble metal is significantly smaller than in the 100°C peak when noble metal is added. When oxygen is deposited on the noble metal catalysts and on reduced ceria via the reaction $2NO \rightarrow N_2 + 2O$, the NO decomposition is inhibited. During repeated NO adsorption/desorption runs the inhibition is slower than expected if the oxygen atoms were deposited as chemisorbed atoms on the surface of noble metal particles, and faster when the dispersion is increased. From these observations we conclude that the oxygen atoms from decomposed NO are incorporated in the bulk and thus cause oxidation of the highly dispersed Pt and Rh particles. Oxygen spillover may also occur but an oxygen spillover effect would not explain the sensitivity of the inhibition effect to dispersion. An O/Pt ratio of 1.5 was observed after oxidation in O_2 at 600°C for Pt/Al_2O_3 samples.

The oxygen "self-poisoning" effect, with respect to NO decomposition, is slower on ceria-supported catalysts, which may be attributed to oxygen spillover from the noble metal to the reduced ceria (*6*); i.e., it takes larger NO exposures to saturate the noble metal particles with oxygen when ceria is present due to a combination of oxygen uptake by the noble metal particles and oxygen spillover to reduced ceria. The reduced ceria-induced effects on the TPD spectra are gradually lost as more and more oxygen is deposited on the catalyst (from dissociated NO or O_2). This suggests that the presence of oxygen vacancies in ceria adjacent to small noble metal particles is responsible for the observed noble metal–ceria interaction.

Oh (*23*) proposed that the observed enhancement of NO dissociation upon ceria addition could be due to the creation of a new adsorption site where the NO molecule is bound via the N atoms to the Rh atoms and the oxygen atoms to reduced ceria particles (the same type of bonding as discussed above for the CO molecule). The decrease in N_2 desorption temperature for the ceria-containing samples may then be associated with NO adsorption on such sites, as this adsorption site should weaken the NO bond and thereby facilitate NO dissociation. Another possible cause is oxygen spillover to oxygen vacancies in ceria, thereby preventing oxygen blocking of sites for NO dissociation.

The kinetics of the reaction $CO + NO \rightarrow CO_2 + \frac{1}{2}N_2$ was found to be enhanced by the addition of ceria. This could be the same effect as in the CO oxidation case, namely that ceria enhances the reaction $CO_a + O_a \rightarrow CO_2$, (where "a" stands for "adsorbed") (*6*). The very low T_{50} values for Rh on ceria-supported catalysts and the correlation between the T_{50} values and the low N_2 desorption temperature may, however, be an indication that different mechanisms are involved in the CO oxidation steps in the two reactions. As mentioned earlier, the reaction studies were not as detailed as the TPD analysis. We therefore only emphasize the clear positive effect of ceria on the CO + NO reaction as observed earlier in the more detailed study by Oh and Eickel (*6*).

In summary we have found that reduced ceria as a support has strong influences on both CO and NO bonding and desorption on Pt and Rh, and on the reaction kinetics for CO oxidation and NO reduction. Further studies on more well-characterized ceria + noble metal samples in combination with surface spectroscopic studies are required to reveal the nature of the ceria–noble metal–adsorbate interactions.

ACKNOWLEDGMENTS

We are grateful to K.-E. Keck for many valuable discussions and to Lars Björnkvist for preparation of the ceria powder samples. Financial support from the National Swedish Board for Technical Development

(contracts STU 89-5405 and STU 87-01446P) is gratefully acknowledged.

REFERENCES

1. Yao, H. C., Japar, S., and Shelef, M., *J. Catal.* **50,** 407 (1977).
2. Den Otter, G. J., and Dautzenberg, F. M., *J. Catal.* **53,** 116 (1978).
3. Summers, J. C., and Ausen, S. A., *J. Catal.* **58,** 131 (1979).
4. Pande, N. K., and Bell, A. T., *J. Catal.* **97,** 137 (1986).
5. Jin, T., Zhou, Y., Mains, G. J., and White, J. M., *J. Phys. Chem.* **91,** 5931 (1987).
6. Oh, S. H., and Eickel, C. C., *J. Catal.* **112,** 543 (1988).
7. Shyu, J. Z., Otto, K., Watkins, W. L. H., Graham, G. W., Belitz, R. K., and Gandhi, H. S., *J. Catal.* **114,** 23 (1988).
8. Engler, B., Koberstein, E., and Schubert, P., *Appl. Catal.* **48,** 71 (1989).
9. Shyu, J. Z., and Otto, K., *J. Catal.* **115,** 16 (1989).
10. Falconer, J. L., and Schwartz, J. A., *Catal. Rev.* **142** (1983).
11. Lööf, P., Kasemo, B., and Keck, K.-E., *J. Catal.* **118,** 339 (1989).
12. Kasemo, B., *Rev. Sci. Instrum.* **50,** 1602 (1979).
13. Lööf, P., Kasemo, B., Björnkvist, L., Andersson, S., and Frestad, A., *in* "Proceedings, 2nd International Congress on Catalysis and Automotive Pollution Control, in press.
14. See, e.g., Kasemo, B., and Törnqvist, E., *Phys. Rev. Lett.* **44,** 23, 1555 (1980); and the references therein.
15. Lööf, P., and Kasemo, B., to be published.
16. Dictor, R., and Roberts, S., *J. Phys. Chem.* **93,** 5846 (1989).
17. Kienneman, A., Breault, R., Hindermann, J. P., and Laurin, M., *J. Chem. Soc., Faraday Trans. 1* **83,** 2119 (1987).
18. Pitchon, V., Primet, M., and Praliaud, H., *Appl. Catal.* **62,** 317 (1990).
19. Yang, A. C., and Garland, C. W., *J. Chem. Phys.* **61,** 1504 (1957).
20. Ichikawa, M., and Fukushima, T., *J. Phys. Chem.* **89,** 1564 (1985).
21. Castner, D. G., and Somorjai, G. A., *Surf. Sci.* **83,** 60 (1979).
22. Jin, T., Okuhara, T., Mains, G. J., and White, J. M., *J. Phys. Chem.* **91,** 3310 (1987).
23. Oh, S. H., *J. Catal.* **124,** 477 (1990).